Oxide/Metal Interface Distance and Epitaxial Strain in the NiO/Ag(001) System

Carlo Lamberti,* Elena Groppo, Carmelo Prestipino, Silvia Casassa, Anna Maria Ferrari, and Cesare Pisani

Department of Inorganic, Physical and Materials Chemistry, University of Torino, Via P. Giuria 7, I-10125 Torino Italy and Unità INFM di Torino, Torino, Italy

Chiara Giovanardi, Paola Luches, and Sergio Valeri

INFM–National Center on nanoStructures and bioSystems at Surfaces (S^3) and Dipartimento di Fisica, Università di Modena e Reggio Emilia, Via G. Campi 213/a, 41100 Modena, Italy

Federico Boscherini

INFM and Dipartimento di Fisica, Università di Bologna, Viale C. Berti Pichat 6/2 40127 Bologna, Italy

(Received 18 March 2003; published 23 July 2003)

Geometric parameters of NiO films epitaxially grown on Ag(001) were determined using two independent experimental techniques and *ab initio* simulations. Primary beam diffraction modulated electron emission experiments determined that the NiO films grow with O on top of Ag and that the oxide/metal interface distance is $d = 2.3 \pm 0.1$ Å. Polarization-dependent x-ray absorption, at the Ni-K edge, determined the tetragonal strain ($r_{\parallel} = 2.046 \pm 0.009$ Å, $r_{\perp} = 2.12 \pm 0.02$ Å) and $d = 2.37 \pm 0.05$ Å. Periodic slab model results agree with the experiments ($d = 2.40$, $r_{\parallel} = 2.07$, $r_{\perp} = 2.10$ Å; the O-on-top configuration is the most stable).

DOI: 10.1103/PhysRevLett.91.046101 PACS numbers: 68.35.–p, 61.10.Ht, 68.55.–a

In recent years, the physical properties of two-dimensional metal-oxide epilayers on metal substrates have become a topic of great interest [1–5]. Films of a few monolayers (ML) can be deposited epitaxially on metal substrates by ultrahigh vacuum techniques, yielding reproducible and well-characterized systems. It has been shown that the energy gap (E_g) of the oxide, in the oxide/metal system, can be modulated by the film thickness T [6–8]. The demonstrated ability to control T represents therefore a new technological opportunity for band-gap engineering. It has also been argued that the presence of the metal substrate can alter significantly the electronic structure of the oxide and influence its chemical properties, with a prospective range of important applications [7]. In the latter respect, *ab initio* simulations of perfect oxide/metal epilayers [9] have given so far a different indication; namely, the electronic structure of the oxide is modified only in a strict vicinity of the interface. The question has therefore been raised whether residual film defectivity could be responsible for the observed enhancement of chemical activity [10–13] and other evidence of modified electronic structure, such as the shift of oxygen core levels, in which case a perfectly epitaxial overlayer would be a poor model of the real systems. We desired therefore to investigate experimentally and theoretically the structure of those systems in order to understand its possible influence in the measured reactivity. This work concerns precisely the comparison between experimental and theoretical estimates of a few critical geometrical parameters of the NiO/Ag(001) system.

For a given oxide/metal system, the structural parameter that establishes the E_g vs T relationship is the oxide/metal interface distance (d). It is so evident that this parameter must be carefully determined in order to design a film with the desired electronic characteristic. In principle, once d has been measured, the E_g vs T relationship is fixed, and so T can be *ad hoc* selected to yield the desired E_g. For the first time, d is here determined for the NiO/Ag(001) system using two independent experimental techniques, primary beam diffraction modulated electron emission (PDMEE) and polarization-dependent x-ray absorption spectroscopy (XAS). The latter technique has also permitted us to obtain accurate estimates of the in-plane and out-of-plane Ni-O bond distances (hereafter $r_{\parallel}$ and $r_{\perp}$, respectively). A periodic slab model has been adopted to calculate quantum mechanically the properties of the NiO/Ag(001) system; the same technique has been used to analyze the effect of tetragonal strain in unsupported NiO films of different thickness.

The NiO films (1, 1.5, 2, 3, and 4 ML thick: 1 ML $\equiv 1.15 \times 10^{15}$ Ni and O) have been grown using Knudsen cells and a directional O_2 flux on the sample ($P_{O_2} = 7 \times 10^{-8}$ Torr) on a Ag(001) substrate previously cleaned by repeated cycles of sputtering (0.6 keV, 1 $\mu A/cm^2$) and annealing (700 K) in UHV. The evaporation rates were measured by means of a quartz crystal microbalance. The film used for XAS has been capped with 5 ML of MgO to avoid surface hydroxylation [14]. A sintered polycrystalline NiO sample, with crystal size in the 500–2000 Å range [13], was used as a reference for XAS.

The structure of the NiO layer, its relationship with the substrate, and the atomic arrangement of the NiO/Ag interface have been investigated by exploiting the modulation of the Auger yield induced by the scattering interference of 5 keV primary electrons [15]. The intensity

angular distributions (IADs) of the Auger Ag MNN, as a function of the incidence angle α of the primary exciting beam, along the high symmetry [110] substrate azimuth, are reported in Fig. 1(a) for different T values. For the clean metal surface, bottom curve, the [001] and [111] features occur at $\alpha_{[hkl]}=0°$ and 54.7°, respectively. In the films, the oxide layers behave as a lens which focuses the primary beam onto the substrate. The d value, and also the in-plane relative position (i.e., adsorption sites), is revealed to strongly influence the IAD of the substrate. In particular, the [111] forward focusing feature shifts to lower angular positions with increasing T. As the first ML of NiO is deposited, the [111] peak becomes more asymmetric and for higher T the maximum itself shifts toward lower angles ($\alpha_{[111]} = 53.1°$ for $T = 4$ ML); as expected $\alpha_{[001]} = 0°$ always. This shift is the consequence of a value of d significantly larger than expected by prolonging the Ag crystal periodicity along the [001] direction ($c/2 = 2.045$ Å) as clearly evidenced by the two schemes in Fig. 1(b): $d = 2.045$ Å $\leftrightarrow \alpha_{[111]} = 54.7°$ (left) and $d > 2.045$ Å $\leftrightarrow \alpha_{[111]} < 54.7°$ (right). The PDMEE patterns have been simulated on the basis of single scattering cluster calculations, which have been successfully used for the MgO/Ag(001) system [15]. Nonstructural parameters have been optimized using the substrate and NiO Auger IAD. Simulation of the Ag IAD was systematically performed for $T = 0, 1, 2, 3$, and 4 ML and for d ranging from 2.0 to 2.6 Å using three different models for the NiO/Ag(001) interface: Ni or O on top of Ag and Ni (and thus O) between two adjacent Ag atoms. The bridge site configuration gave a high discrepancy with the measured IAD and was thus excluded. Figure 1(c) reports the simulated $\alpha_{[111]}$ value vs T, for three different values of d (2.086, 2.30, and 2.50 Å, ▲, ★, and ■ symbol, respectively), in the O-on-top model. We can notice that the position of the $\alpha_{[111]}$ peak depends on both d and T. The sensitivity in the determination of d through the measurement of $\alpha_{[111]}$ is higher for $T = 3$ and 4 ML. Therefore, the $T = 4$ ML IAD has been simulated for both O- and Ni-on-top models, with d in the 2.0–2.60 Å range, sampled each 0.05 Å. The systematic comparison among the so obtained r factors, a measure of the quality of the fit [see Fig. 1(d)], allows us to establish that the O-on-Ag configuration (▼ data) is the preferred one and to quantify the interface distance: $d = 2.3 \pm 0.1$ Å.

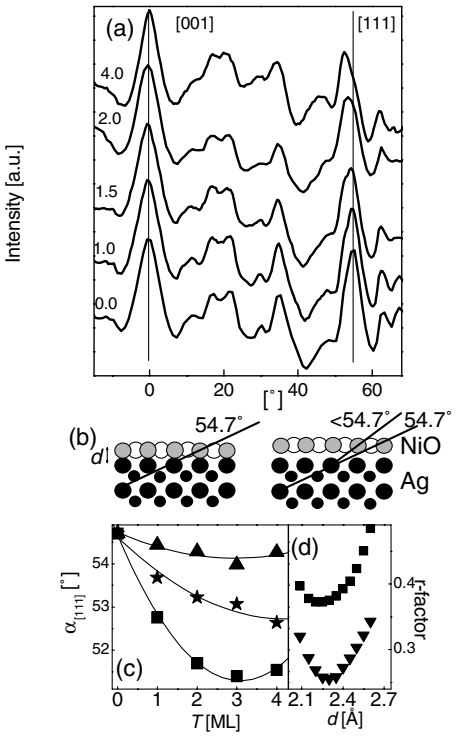

FIG. 1. (a) IAD of Ag MNN electrons along the [110] azimuth for increasing NiO thickness (from bottom to top $T =$ 0.0, 1.0, 1.5, 2.0, and 4.0 ML). Main forward focusing features are indicated. (b) Schematic representation of the NiO/Ag(001) system (O-on-top model) along the [110] azimuth for unexpanded ($d = 2.045$, left) and expanded ($d > 2.045$, right) interfacial distances. Gray and white spheres represent O and Ni atoms, while big and small black spheres are Ag atoms located at two parallel planes shifted by $a/(2\sqrt{2})$. (c) Simulated [111] peak vs film thickness T, for $d = 2.086$, 2.30, and 2.50 Å, ▲, ★, and ■ symbols, respectively. (d) r factors vs d for the 4 ML thick film assuming either the O-on-Ag (▼) or the Ni-on-Ag (■) configurations as model.

Ni-K edge XAS has then been used to improve the accuracy of d determination and to measure the tetragonal distortion of the pseudomorphic NiO films. The polarization dependence of the XAS cross section allows structural determination with directional sensitivity. By exploiting the linear polarization of the synchrotron beam and by orienting the sample with the surface either parallel or perpendicular to the electric vector of the impinging radiation, it is possible to preferentially probe in-plane or out-of-plane atomic correlations [16]. XAS data have been collected at the GILDA BM8 beam line, at the European Synchrotron Radiation Facility (Grenoble, France) using a dynamically focused double crystal Si(311) monochromator. For the NiO film ($T = 3$ ML) the fluorescence mode (13 element hyperpure Ge detector) has been used, while the sintered NiO reference sample was measured in the transmission mode. The film was measured in normal and grazing incidence geometries. The data processing was performed with a multiple scattering (MS) approach, since MS paths have significant amplitude in the rock-salt structure [14,17,18]. Theoretical phase shifts and amplitudes were generated by means of the FEFF 8.10 code [19] taking polarization into account.

The k^3-weighted Fourier transforms (FTs) of the XAS data are reported in Fig. 2 (● and ▲ symbols for the modulus and the imaginary part, respectively). A strong damping of the intensity of the XAS signal is observed by moving from normal to grazing angle geometry (top vs bottom curves in Fig. 2). This is due to both (i) a reduction

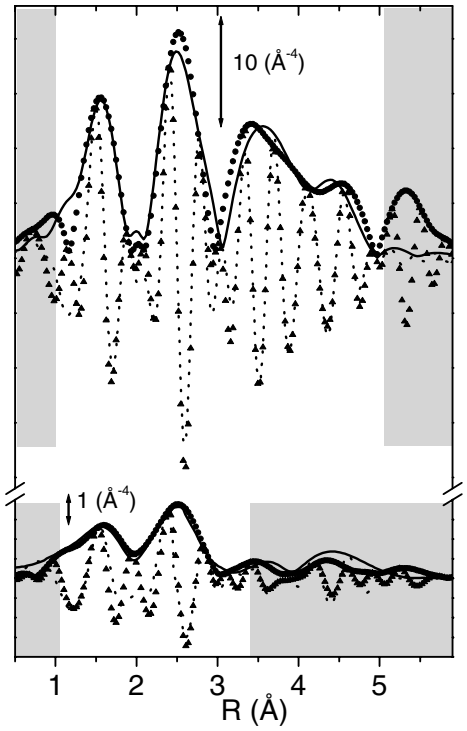

FIG. 2. Modulus (full line) and imaginary part (dashed line) k^3-weighted, phase uncorrected, FTs of the experimental $\chi(k)$ functions of a $T = 3$ ML NiO/Ag(001) film compared with the modulus (scattered dots) and the imaginary part (scattered triangles) of the corresponding best fits. Top and bottom curves refer to data collected at normal and glancing geometries, respectively. White and gray-dashed parts differentiate the R region where the experimental data have been fitted to those excluded from the fitting procedure.

of the actual number of neighbor atoms in the direction perpendicular to the film and (ii) a significant increase of the Debye-Waller factors of static origin most probably due to a spread of local structures (e.g., deviation from ideal 2D growth resulting in island formation, where edge and corner positions are available for Ni atoms). The experimental curves were fitted, using the FEFFIT 2.55 code, in the 1.0–5.1 Å and 1.0–3.4 Å ranges for normal and grazing geometries, respectively, which include contributions up to the sixth and to the third coordination shells around Ni, respectively. Simulations have been performed on the basis of an ideal tetragonal distortion of the film, resulting in a uniform contraction of the in-plane distances and uniform elongation of the out-of-plane ones [17]. The best fits, also reported in Fig. 2 (full and dashed lines for the modulus and the imaginary part, respectively), resulted in the following estimates: $r_{\parallel} = 2.046 \pm 0.009$ Å, $r_{\perp} = 2.12 \pm 0.02$ Å, to be compared with the $r = 2.092 \pm 0.004$ Å estimate obtained for the bulk polycrystalline reference sample and with the x-ray diffraction (XRD) value (2.088 Å). The fit of the spectrum collected in grazing angle geometry has been obtained with a Ni-Ag contribution at a distance of 3.13 ± 0.04 Å. According to the PDMEE model of a NiO/Ag(001) interface in which the O atoms are located on top of Ag atoms, the measured Ni-Ag distance implies that $d = 2.37 \pm 0.05$ Å. This value is expanded if compared to both NiO and Ag half lattice parameters (2.088 and 2.045 Å, respectively) and is in agreement with the PDMEE value.

To validate the picture emerging from PDMEE and XAS experimental data, we have performed periodic *ab initio* calculations with a β version of the CRYSTAL code [20]. The model adopted and the computational techniques are as in a previous paper [21] to which reference can be made for all computational details. The supported film was simulated by a two-dimensionally periodic slab of five layers of silver atoms parallel to the (001) face, epitaxially covered on both sides with 1 ML of NiO. A hybrid-exchange Hamiltonian was adopted because of its satisfactory performance in describing the bulk properties of both silver and nickel oxide, and a basis set of triple-zeta quality was used for all atoms. The equilibrium geometry of the substrate and that of an epitaxial NiO monolayer were there determined. In particular, the O-on-top configuration was found more stable than the Ni-on-top one (in agreement with PDMEE results) by 0.25 eV/NiO unit. The former configuration has been adopted in the present study, which concerns the case $T = 2$ ML; thicker substrates or epilayers are presently not feasible, because of computational costs and numerical convergence problems. The z coordinates of all atoms of the oxide have been optimized either by forcing Ni and O atoms to lie on the same plane (*flat* data) or without constraints (*free* data) [21]. Because of the assumption of perfect epitaxy, the lattice parameter of the overlayer parallel to the crystal face has been forced to coincide with the optimized one for the silver support ($a/2 = 2.07$ Å, experimentally, $a/2 = 2.045$ Å), while the optimized NiO bulk value is $a/2 = 2.10$ Å (experimentally, $a/2 = 2.09$ Å). Comparison of the present results with those for $T = 1$ ML [21] confirms that the electronic structure of the oxide is modified only in a strict vicinity of the interface, in agreement with the main conclusions drawn from a similar study of silver supported epitaxial MgO films of different T [9]. The presence of an oxide layer above the first one has the effect of reducing the corrugation of the first oxide layer, because of attraction exerted by O anions in the second layer on Ni cations, and of reducing the interaction energy between metal and oxide. The electronic structure (electron and spin populations, position of the Fermi level, etc.) are hardly modified. The energetic and geometric features when passing from $T = 1$ to $T = 2$ ML are as follows (the *flat* values are in parentheses): interaction energy per NiO unit from 0.25 (0.23) eV to 0.21 (0.18) eV; distance between O and Ag surface from 2.44 (2.44) Å to 2.46 (2.46) Å; d from 2.36 (2.44) Å to 2.40 (2.46) Å. $r_{\parallel}$ has been constrained to 2.07 Å while $r_{\perp}$, meaningful for $T = 2$ ML only, is 2.10 (2.07) Å. The 2.10 Å value, obtained in the *free* case, corresponds to the average

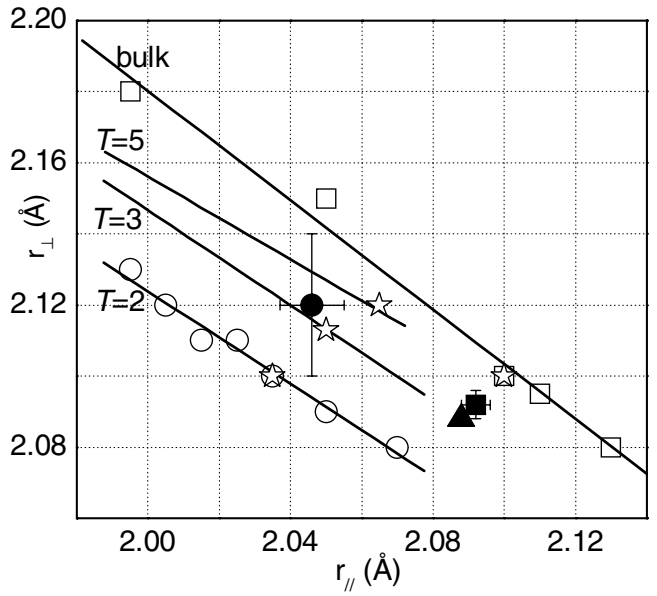

FIG. 3. Relation between out-of-plane and in-plane NiO distances ($r_\perp$; $r_\parallel$) for unsupported NiO films of different thicknesses T. For $T = 2$ (open circles) and $T = \infty$ (open squares) we report the calculated points to give an idea of data dispersion. For clarity, only the best linear fits are reported for $T = 3$ and 5. Open stars indicate the calculated equilibrium configurations $[r^*_\perp(T); r^*_\parallel(T)]$ for each T value. The full dot and the full square represent the experimental values for $T = 3$ and ∞, respectively, as determined by XAS, the latter being compatible with the XRD datum (full triangle).

between the O_1-Ni_2 (2.07 Å) and Ni_1-O_2 (2.13 Å) distances, where the suffix (1 or 2) reflects the NiO layer from the Ag surface (first or second). $d = 2.40$ Å, obtained for $T = 2$ ML, *free* case, is in excellent agreement with the Ni-K edge XAS value, $d = 2.37 \pm 0.05$ Å. We do not believe that this theoretical result could be altered by considering thicker overlayers.

In order to check how far the constraint of perfect epitaxy may influence the tetragonal distortion of the overlayer, we have studied with the same theoretical approach unsupported NiO films, with $T = 2, 3, 5, \ldots, \infty$, and determined both their equilibrium configuration $[r^*_\perp(T); r^*_\parallel(T)]$ and the optimum value of $r_\perp$, for $r_\parallel$ fixed to $a/2 = 2.07$ Å; see Fig. 3. Very thin films are considerably contracted in the parallel direction with respect to the bulk value: $r^*_\parallel(T) = 1.98, 2.03, 2.055, 2.07, 2.10$ Å, for $T = 1, 2, 3, 5, \infty$. Perpendicular deformation is comparatively less important: $r^*_\perp(T) = 2.10, 2.115, 2.12, 2.10$ Å, for $T = 2, 3, 5, \infty$. Let us define $\varepsilon(T) = [r^*_\parallel(T) - a/2]/(a/2)$; then previous considerations would imply that $\varepsilon(T)$ changes its sign by increasing T [$\varepsilon(T) < 0$ for $T < 3$ ML, $\varepsilon(T) > 0$ for $T > 5$ ML], being practically zero for $T = 3$ to 5 ML. In this range, the tetragonal distortion for the supported and unsupported film is about the same. This could justify the excellent agreement between calculated and experimental results for $T =$ 3 ML, also shown in Fig. 3. Incidentally, it may be noted that the calculated distance $r^*_\perp(2$ ML) is the same as the average distance between the two layers in the epitaxial bilayer (2.10 Å). Another interesting outcome of the calculations is the response to tetragonal strain. The slope of the $r_\perp(r_\parallel)$ curves is in the range -0.60– -0.77; the latter is the value for the bulk, in fair agreement with the experimental γ value for NiO (-0.844) [22].

In conclusion, the present study has provided, for the first time, accurate estimates of geometric parameters concerning the NiO/Ag(001) metal-oxide interface. The comparison between results obtained with two independent experimental techniques and with *ab initio* calculations is excellent. Therefore, the high reactivity of oxide films experimentally observed and never reproduced theoretically cannot be ascribed to significant difference in the structure of real systems and their theoretical models.

This work has been funded by INFM under PRA-ISADORA and Commissione Luce di Sincrotrone. We are indebted to the staff of GILDA BM8 beam line for excellent support during XAS measurements.

*Electronic address: carlo.lamberti@unito.it

[1] H. J. Freund, Angew. Chem., Int. Ed. Engl. **36**, 452 (1997).
[2] D. A. Muller *et al.*, Phys. Rev. Lett. **80**, 4741 (1998).
[3] H. L. Meyerheim *et al.*, Phys. Rev. Lett. **87**, 076102 (2001).
[4] S. Schintke *et al.*, Phys. Rev. Lett. **87**, 276801 (2001).
[5] Y. T. Matuvich, T. J. Vink, and P. A. Z. van Emmichoven, Phys. Rev. Lett. **89**, 167601 (2002).
[6] S. Altieri, L. H. Tjeng, and G. A. Sawatzky, Phys. Rev. B **61**, 16 948 (2000).
[7] S. Altieri, L. H. Tjeng, and G. A. Sawatzky, Thin Solid Films **400**, 9 (2001).
[8] D. M. Duffy, J. H. Harding, and A. M. Stoneham, Acta Metall. Mater. **43**, 1559 (1995).
[9] M. Sgroi, C. Pisani, and M. Busso, Thin Solid Films **400**, 64 (2001).
[10] C. Di Valentin *et al.*, J. Phys. Chem. B **106**, 11 961 (2002).
[11] C. Di Valentin *et al.*, J. Phys. Chem. B **106**, 7666 (2002).
[12] G. Pacchioni, Surf. Rev. Lett. **7**, 277 (2000).
[13] A. Zecchina *et al.*, Adv. Catal. **46**, 265 (2001).
[14] P. Luches *et al.*, Nucl. Instrum. Methods Phys. Res., Sect. B **200**, 371 (2003).
[15] S. Valeri and A. di Bona, Surf. Rev. Lett. **4**, 141 (1997); C. Giovanardi *et al.*, Surf. Sci. **505**, L209 (2002).
[16] M. Tormen *et al.*, Phys. Rev. B **63**, 115326 (2001).
[17] E. Groppo *et al.*, J. Phys. Chem. B **107**, 4597 (2003).
[18] A. Corrias, G. Mountjoy, G. Piccaluga, and S. Solinas, J. Phys. Chem. B **103**, 10 081 (1999).
[19] A. L. Ankudinov *et al.*, Phys. Rev. B **58**, 7565 (1998).
[20] V. R. Saunders *et al.*, CRYSTAL98 User's Manual, University of Torino, 1998.
[21] S. Casassa *et al.*, J. Phys. Chem. B **106**, 12 978 (2002).
[22] P. de V. du Plessis, S. J. van Tonder, and L. Alberts, J. Phys. C **4**, 1983 (1971).